AMERICAN SOCIETY FOR MICROBIOLOGY | Infection and Immunity

Distinct Roles of Myosins in *Aspergillus fumigatus* Hyphal Growth and Pathogenesis

Hilary Renshaw,[a] José M. Vargas-Muñiz,[a] Amber D. Richards,[b] Yohannes G. Asfaw,[c] Praveen R. Juvvadi,[b] William J. Steinbach[a,b]

Department of Molecular Genetics and Microbiology, Duke University Medical Center, Durham, North Carolina, USA[a]; Division of Pediatric Infectious Diseases, Department of Pediatrics, Duke University Medical Center, Durham, North Carolina, USA[b]; Division of Laboratory Animal Resources, Duke University Medical Center, Durham, North Carolina, USA[c]

Myosins are a family of actin-based motor proteins found in many organisms and are categorized into classes based on their structures. Class II and V myosins are known to be important for critical cellular processes, including cytokinesis, endocytosis, exocytosis, and organelle trafficking, in the model fungi *Saccharomyces cerevisiae* and *Aspergillus nidulans*. However, the roles of myosins in the growth and virulence of the pathogen *Aspergillus fumigatus* are unknown. We constructed single- and double-deletion strains of the class II and class V myosins in *A. fumigatus* and found that while the class II myosin (*myoB*) is dispensable for growth, the class V myosin (*myoE*) is required for proper hyphal extension; deletion of *myoE* resulted in hyperbranching and loss of hyphal polarity. Both *myoB* and *myoE* are necessary for proper septation, conidiation, and conidial germination, but only *myoB* is required for conidial viability. Infection with the Δ*myoE* strain in the invertebrate *Galleria mellonella* model and also in a persistently immunosuppressed murine model of invasive aspergillosis resulted in hypovirulence, while analysis of bronchoalveolar lavage fluid revealed that tumor necrosis factor alpha (TNF-α) release and cellular infiltration were similar compared to those of the wild-type strain. The Δ*myoE* strain showed fungal growth in the murine lung, while the Δ*myoB* strain exhibited little fungal burden, most likely due to the reduced conidial viability. These results show, for the first time, the important role these cytoskeletal components play in the growth of and disease caused by a known pathogen, prompting future studies to understand their regulation and potential targeting for novel antifungal therapies.

In filamentous fungi, the actin cytoskeleton is critical for a myriad of important cellular functions, including cytokinesis, hyphal-tip growth, endocytosis, and exocytosis (1–7). Myosins are involved in many of these roles by their interaction with actin microfilaments. The number of myosins varies greatly between organisms; however, fungi contain relatively few myosins in comparison to humans (8). Myosins have been studied in the model fungi *Saccharomyces cerevisiae* and *Aspergillus nidulans*,(1, 3, 9–15), but not in the pathogen *Aspergillus fumigatus*. *S. cerevisiae* contains five myosin-encoding genes encompassing three classes (16–20), while the filamentous fungus *A. nidulans* possesses four classes of myosins: class I, class II, class V, and the fungus-specific class XVII, which contains a myosin motor head and a chitin synthase domain (1, 5, 14). The conventional myosins, class II myosins, have a role in cytokinesis through involvement in the cytokinetic actomyosin ring (CAR) (21). Deletion of the class II myosins in *Talaromyces* (formerly Penicillium) *marneffei* and *A. nidulans* led to cytokinesis defects or septation failure (5, 22). In addition, mutants lacking the sole class II myosin in *A. nidulans* (MyoB) exhibited a lack of conidiation, extreme growth defects, and improper chitin deposition (5). Further supporting its role in septation, *A. nidulans* MyoB transiently localized to the septum as nodes or strings (5).

Class V myosins are vesicle transporters and are important for maintaining cell polarity (5, 13, 19, 23, 24). The *S. cerevisiae* genome encodes two class V myosins, one of which is essential (Myo2p) (18, 23). Mutation of *myo2* leads to enlarged and unbudded cells with accumulation of secretory vesicles (19, 23). Similarly, deletion of the class V myosin in *Candida albicans* leads to unbudded large cells that do not form germ tubes or hyphae (25). Deletion of the class V myosin in the plant-pathogenic fungus *Ustilago maydis* decreases virulence in maize plants (26). In *A. nidulans*, the sole class V myosin (MyoE) is not essential but is required for proper vesicle trafficking to the Spitzenkörper in an actin-dependent manner (5). *A. nidulans* MyoE localized to the Spitzenkörper, in dot-like structures throughout the hyphae, and transiently at the septa under its native promoter (5, 7). However, under the control of a regulatable promoter, MyoE was shown to localize stably to both sides of the septa (7). Deletion of *myoE* in *A. nidulans* led to morphologically normal septa that were closer together (7); however, the function of the class V myosin in this process is currently unknown. The known roles of myosins in critical cellular processes, including hyphal-tip growth and cytokinesis, make them likely to be crucial for cellular functions related to pathogenesis.

Despite the established functions of myosins in other fungi, their roles in the pathogen *A. fumigatus* have not been established. In this study, we characterized the class II (MyoB) and class V (MyoE) myosins of *A. fumigatus* and their roles in hyphal growth and virulence by generating single deletions of both *myoB*

Received 17 September 2015 **Returned for modification** 5 October 2015
Accepted 24 February 2016

Accepted manuscript posted online 7 March 2016

Citation Renshaw H, Vargas-Muñiz JM, Richards AD, Asfaw YG, Juvvadi PR, Steinbach WJ. 2016. Distinct roles of myosins in *Aspergillus fumigatus* hyphal growth and pathogenesis. Infect Immun 84:1556–1564. doi:10.1128/IAI.01190-15.

Editor: G. S. Deepe, Jr.

Address correspondence to William J. Steinbach, bill.steinbach@duke.edu.

Supplemental material for this article may be found at http://dx.doi.org/10.1128/IAI.01190-15.

TABLE 1 Strains used in this study

Strain	Parent strain	Genotype	Reference or source
akuB^{KU80}	CEA17	Wild type	46
akuB^{KU80} *pyrG*$^{-}$	CEA17 *pyrG*$^{+}$	*pyrG*	46
Δ*myoB*	*akuB*^{KU80} *pyrG*$^{-}$	Δ*myoB*::*pyrG*	This study
Δ*myoE*	*akuB*^{KU80} *pyrG*$^{-}$	Δ*myoE*::*pyrG*	This study
Δ*myoB* Δ*myoE*	Δ*myoB*	Δ*myoB*::*pyrG* Δ*myoE*::*ble*	This study
myoB-egfp	*akuB*^{KU80}	*myoB*::*myoBpromo-myoB-egfp-hph*	This study
myoE-egfp	*akuB*^{KU80}	*myoE*::*myoEpromo-myoE-egfp-hph*	This study

(Δ*myoB*) and *myoE* (Δ*myoE*), as well as a double-deletion strain (Δ*myoB* Δ*myoE*). While the deletion of *myoB* resulted in aberrant septation and reduced conidiation, the deletion of *myoE* caused a significant growth defect, hyperseptation, hyperbranching, loss of hyphal polarity, and loss of conidiation. Deletion of both *myoB* and *myoE* resulted in a more severe phenotype. The Δ*myoE* strain displayed attenuated virulence in a *Galleria mellonella* model and in a murine intranasal model of invasive aspergillosis and similarity in tumor necrosis factor alpha (TNF-α) release and cellular infiltration in comparison to infection with the wild-type strain. Although the Δ*myoB* strain showed decreased mortality in both animal models and a significant reduction in TNF-α release, this was most likely due to the reduced conidial viability and therefore decreased fungal burden.

MATERIALS AND METHODS

Strains, media, and culture conditions. The strains used in this study are listed in Table 1. The *A. fumigatus akuB*^{KU80} and *akuB*^{KU80} *pyrG*$^{-}$ uracil/uridine auxotrophic strains were used for deletion analyses, and the *A. fumigatus akuB*^{KU80} strain was used as the wild-type reference strain. Cultures were grown on glucose minimal medium (GMM) supplemented with 5 mM uracil and 5 mM uridine (GMM plus UU) at 37°C, except where otherwise specified. *Escherichia coli* DH5α competent cells were used for cloning.

Construction of myosin deletion and green fluorescent protein (GFP)-tagged strains. The primers used are listed in Table S1 in the supplemental material. Both the Δ*myoB* and the Δ*myoE* strains were generated by replacing each gene with *pyrG* from *Aspergillus parasiticus*. Approximately 1 kb upstream and downstream of each gene was PCR amplified from *A. fumigatus* AF293 genomic DNA and cloned into the pJW24 vector (27). The resulting plasmids were linearized with SalI and SacI to obtain the deletion cassette (approximately 5.5 kb for *myoB* and 5.2 kb for *myoE*) and transformed into an *akuB*^{KU80} *pyrG*$^{-}$ auxotrophic strain as previously described (27). Transformants were selected for growth in the absence of uracil/uridine. To construct the double-deletion strain, the pBlue-phleo plasmid was constructed by digesting pBlueScript II and pUCnGPhleo (28) with HindIII and ligating the *ble* cassette into pBlueScript II. Approximately 1 kb of upstream and downstream sequence of *myoE* was PCR amplified from AF293 genomic DNA and cloned into pBlue-phleo. The resulting plasmid was used as a template for final PCR amplification for transformation. The 5-kb PCR product was transformed into the Δ*myoB* strain, and transformants were selected in the presence of phleomycin (125 μg/ml). Deletions were confirmed by PCR and/or Southern analysis. The *myoB-egfp* expression strain was generated by cloning approximately 1 kb of a partial *myoB* gene and 1 kb of *myoB* terminator sequence into the pUCGH vector (29). The resulting plasmid was linearized with KpnI and HindIII and transformed into the *akuB*^{KU80} strain. The *myoE-egfp* strain was generated by cloning approximately 1 kb of a partial *myoE* gene and 1 kb of *myoE* terminator sequence into pUCGH. The resulting plasmid was linearized with KpnI and XbaI and transformed into the *akuB*^{KU80} strain. Transformants were selected by growth in the presence of hygromycin B (150 μg/ml).

Radial growth, conidium harvesting, and quantification. Conidia (10^4) were inoculated on GMM-plus-UU or sorbitol minimal medium (SMM) agar and incubated at 37°C, and radial growth was measured every 24 h for 5 days. To quantify conidium production, 10^4 conidia were inoculated onto GMM-plus-UU or SMM agar, incubated at 37°C for 5 days, harvested in 10 ml 0.05% Tween 80, and quantified using a hemacytometer as previously described (30). All assays were performed in triplicate. The mean growth rates for each of the strains were compared statistically by Student's *t* test using GraphPad Prism (San Diego, CA). To obtain conidia for experimentation, conidia (10^4) were inoculated onto SMM; grown for 5 days at 37°C, with the exception of the Δ*myoB* Δ*myoE* strain, which was grown for 14 days to allow sufficient conidium production; and harvested in 10 ml 0.05% Tween 80. The harvested conidia were diluted and stored at 4°C in water.

Fluorescence and transmission electron microscopy (TEM). For fluorescence microscopy, conidia (10^4) were inoculated and cultured for 18 h at 37°C in 60- by 15-mm petri dishes containing coverslips (22 by 40 mm; no. 1) immersed in 5 ml liquid GMM. The strains were observed using an Axioskop 2 plus microscope (Zeiss) equipped with AxioVision 4.6 imaging software.

For TEM of hyphae, conidia were inoculated into 10 ml GMM and incubated at 37°C for 24 h to generate hyphae. For TEM of conidia and hyphae, samples were centrifuged at 2,000 rpm for 5 min, and the supernatant was removed. Samples were washed twice with phosphate-buffered saline (PBS) for 10 min, stained for 1 h with osmium tetroxide, and washed twice with PBS and once with 0.1 N acetate buffer for 10 min. The samples were stained with 0.5% uranyl acetate for 1 h; washed twice for 10 min each time using 0.1 N acetate buffer; and dehydrated using serial washes of 30%, 50%, 70%, 90%, and 100% ethanol twice for 10 min each time at each concentration. The samples were embedded using the Spurr Low Viscosity Embedding kit and were thin sectioned and stained using 1% uranyl acetate and 0.4% lead citrate. Hyphae were visualized using an accelerating voltage of 80 kV on a FEI Tecnai G^2 Twin.

Aniline blue and calcofluor white staining and apical/subapical-compartment measurements. Conidia (10^4) of each strain were cultured in 60- by 15-mm petri dishes with coverslips immersed in 5 ml of GMM-plus-UU broth and incubated for 18 h at 37°C (28). For aniline blue staining, the coverslips were rinsed with GMM-plus-UU broth, inverted over 500 μl of aniline blue stain, and incubated for 5 min at 25°C. The coverslips were rinsed briefly with GMM-plus-UU broth and observed by fluorescence microscopy. For calcofluor white staining, coverslips were washed in 50 mM PIPES [piperazine-*N*,*N*′-bis(2-ethanesulfonic acid)] (pH 6.7) for 5 min, fixed in 8% formaldehyde for 1 h at 25°C, washed twice in 50 mM PIPES (pH 6.7) for 10 min at 25°C, and then treated with 100 μg/ml RNase for 60 min at 37°C. Samples were then stained with 1 μg/ml calcofluor white in 500 μl of PIPES (pH 6.7) for 5 min and visualized under a fluorescence microscope.

To determine the apical- and subapical-compartment measurements, conidia (10^4) were cultured on coverslips immersed in 5 ml of GMM-plus-UU broth, incubated for 18 h at 37°C (28), and then stained with aniline blue as described above and visualized using fluorescence microscopy. The apical compartment was measured from the apex of the hyphae to the apical septum. The subapical compartment was measured from the

apical septum to the subapical septum. Statistical analysis was performed using Student's *t* test comparing wild-type strain apical versus Δ*myoE* strain apical lengths and wild-type-strain subapical versus Δ*myoE* strain subapical lengths.

Antifungal susceptibility testing. Conidia (10^4) were inoculated on GMM-plus-UU agar supplemented with either caspofungin (1 or 4 μg/ml) or nikkomycin Z (2 μg/ml), and growth was visualized after 5 days at 37°C. For liquid culture, conidia (100 μl of 2×10^4 conidia/ml) were inoculated into RPMI medium according to CLSI standards and supplemented with the appropriate concentrations of caspofungin, and growth was monitored for 48 h to determine the minimum effective concentration (MEC) of the anti-cell wall agent for the strains (31, 32).

***G. mellonella* and murine invasive aspergillosis animal models.** As initial virulence screening in the invertebrate *G. mellonella* invasive aspergillosis infection model, 20 larvae were infected with 5 μl of a suspension of 1×10^8 conidia/ml. Infected larvae were incubated at 37°C, and survival was scored daily for 5 days (27). For the murine model of invasive aspergillosis, male CD1 mice (Charles River Laboratories, Raleigh, NC) were immunosuppressed with cyclophosphamide (175 mg/kg of body weight intraperitoneally on days −2 and +3), and triamcinolone acetonide (40 mg/kg subcutaneously on days −1 and +6), and intranasal infection of 20 mice per strain was performed on day 0 with 40 μl of 10^8 conidia/ml; The mice were monitored daily for survival for 14 days (33). Survival for the invertebrate and murine models was plotted on a Kaplan-Meier curve with log rank pairwise comparison. Statistical significance was defined as a two-tailed *P* value of <0.05.

Histopathology of murine lungs. Three additional mice per strain were subjected to histological examination. The mice were euthanized at day +3 after infection, the lungs were harvested, and tissues (5-μm sections) were stained with Gomori's methenamine silver stain and hematoxylin and eosin (H&E) stain (27).

Bronchoalveolar lavage, ELISA, and flow cytometry analysis. Five additional mice per strain were immunosuppressed and infected as described above with water used for mock infection. On day +3, bronchoalveolar lavage fluid (BALF) was collected by instilling the lungs with 5 ml PBS containing 0.05 M EDTA. The first 1 ml collected was centrifuged, and the supernatant was removed for TNF-α quantification by enzyme-linked immunosorbent assay (ELISA). The cell pellet was added to the other 4 ml of BALF collected. TNF-α release was measured using the Mouse TNF-α ELISA Max Standard kit (BioLegend) following the manufacturer's instructions. For flow cytometric analysis of BALF cells, single-cell BALF suspensions were washed and stained with antibodies specific for the following cell surface markers: CD115 and Ly6C (eBioscience, San Diego, CA); CD11b, CD11c, CD24, CD31, IA/IE, Ly6G, and Siglec-F (BD Biosciences, San Jose, CA); and CD3, CD45, CD64, CD103, B220, and F4/80 (BioLegend, San Diego, CA). One channel was used to detect autofluorescence. In addition, Zombie Yellow LIVE/DEAD (Biolegend, San Diego, CA) was used to exclude dead cells. Data were collected with a BD LSR II flow cytometer and analyzed with FlowJo software. Single cells were identified using forward and side scatter, dead cells were excluded, and leukocytes were identified as $CD45^+$ cells. Neutrophils were identified as $CD45^+$ $Ly6G^+$ cells, and alveolar macrophages were identified as $CD45^+$ $Ly6G^-$ $CD64^+$ Siglec-F^+ cells. For ELISA and flow cytometry, statistical significance ($P < 0.05$) was determined using an unpaired *t* test comparing the wild-type strain to the deletion strains.

Germination and conidial viability. Conidia (~100) were inoculated into 5 ml GMM in 60- by 15-mm petri plates in triplicate and incubated at 37°C. Fifty conidia were quantified per plate every hour for 18 h and then again at 24-h, 36-h, and 48-h time points for the double-deletion strain using a Nikon Diaphot phase-contrast microscope. Conidia were considered germinated when a germ tube was visible. The statistical differences for the groups at the 18-h time point were determined pairwise by the chi-square test.

To obtain conidia for viability staining, conidia (10^4) were inoculated onto SMM, grown for 5 days at 37°C, and harvested in 10 ml water or PBS. The harvested conidia were diluted and stored at 4°C in water or PBS for 4 days. For viability staining, conidia (10^4) were centrifuged at 13,000 rpm for 2 min, and the supernatant was removed. Bis-(1,3-dibutylbarbituric acid) trimethine oxonol (DiBAC) (2 μg/ml in 100 mM MOPS [morpholinepropanesulfonic acid], pH 7.0) was added to the conidia to stain them, samples were vortexed and incubated in the dark at room temperature for 1 h and then centrifuged at 13,000 rpm for 2 min, the supernatant was removed, and the conidia were washed twice with 100 mM MOPS, pH 7.0 (34). Carboxyfluorescein diacetate (CFDA) (50 μg/ml in 100 mM MOPS, pH 3.0) was added to the conidia, and samples were vortexed and incubated in the dark for 45 min at 37°C with gentle agitation. The stained conidia were visualized using an Axioskop 2 plus microscope (Zeiss) with a GFP filter. Fifty conidia were counted three times per strain and marked as viable or nonviable. The statistical significance ($P < 0.05$) was determined using an unpaired *t* test comparing the wild-type strain to the deletion strains or multiple *t* tests to compare water- versus PBS-harvested conidia.

RESULTS

Deletion of *myoB* or *myoE* results in abnormal colony morphology, conidiation defects, septation, and cell wall component localization. To investigate the role of myosins in *A. fumigatus*, we generated single-deletion strains (Δ*myoB* and Δ*myoE*) and a double-deletion strain (Δ*myoB* Δ*myoE*) (see Fig. S1A and B in the supplemental material). While the Δ*myoB* strain showed radial growth comparable to that of the wild-type strain, the Δ*myoE* strain and the Δ*myoB* Δ*myoE* strain each showed a significant defect in radial growth ($P < 0.000001$ for both at day 5) (Fig. 1D). Under differential interference contrast microscopy, the Δ*myoE* strain and the Δ*myoB* Δ*myoE* strain displayed hyperbranching and loss of polarity (Fig. 1A and B), while the Δ*myoB* strain appeared normal.

All three myosin deletion strains grew as white colonies on GMM, which could indicate a lack of conidiation (Fig. 1A and B). Quantification of conidial production showed that the Δ*myoB* strain resulted in a >99% decrease in conidiation ($P < 0.0001$) compared to the wild-type strain grown in GMM. The Δ*myoE* and Δ*myoB* Δ*myoE* strains completely lacked conidia. The conidiation defect was partially remediated in each mutant strain in the presence of sorbitol (data not shown); however, the remediated Δ*myoB* Δ*myoE* strain produced conidia only after 14 days of growth. Quantification of conidial production when grown in the presence of sorbitol showed that the Δ*myoB* strain produced numbers of conidia equal to those of the wild-type strain ($P > 0.05$), while the Δ*myoE* strain exhibited a nearly 75% decrease ($P < 0.01$) and the Δ*myoB* Δ*myoE* strain exhibited a >80% decrease ($P < 0.01$) in comparison to the wild-type strain.

Previous studies in *A. nidulans* showed that deletion of *myoB* or *myoE* affected septation, and therefore, we used aniline blue, which selectively stains cell wall β-(1,3)-glucan, and found that deletion of *myoB* abolished nearly all septation, and any septa that could be visualized possessed either central or lateral defects in septation leading to abnormal septal closure. They included septa extending from both sides of the hyphae but not meeting centrally and septa extending from only one side (Fig. 1A). Conversely, deletion of *myoE* resulted in hyperseptation, but with normal septal morphology. However, the double-deletion strain showed aberrantly formed, incomplete septa and irregular β-(1,3)-glucan deposition (Fig. 1B). The myosin deletion strains were also stained with calcofluor white to visualize chitin. The Δ*myoB* strain showed irregular accumulation of chitin, as was observed with

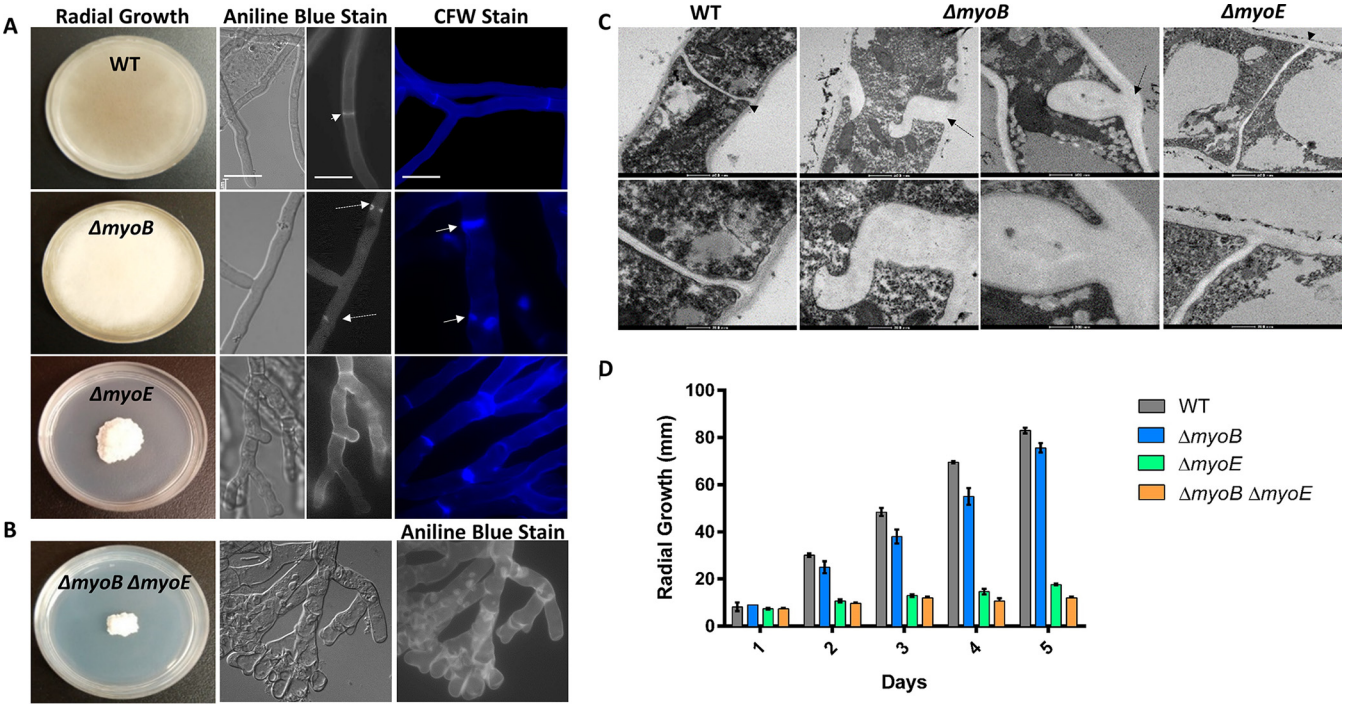

FIG 1 Myosins are required for proper hyphal and septal morphology. (A) Deletion of *myoB* resulted in white colonies with wild-type (WT) radial growth. Deletion of *myoE* resulted in white, compact colonies. Conidia (10^4) were spotted onto GMM agar and incubated for 5 days at 37°C. Single deletion of *myoB* resulted in β-(1,3)-glucan mislocalization, and deletion of *myoB* or *myoE* resulted in chitin mislocalization. Conidia (10^4) were inoculated into 5 ml GMM on sterile coverslips for 18 h at 37°C. The coverslips were stained with aniline blue to stain β-glucan or calcofluor white (CFW) to stain chitin and were visualized using fluorescence microscopy. The arrowhead indicates a normal septum, the dashed arrows indicate β-(1,3)-glucan mislocalization, and the solid arrows indicate chitin mislocalization. Bar, 10 μm. (B) Strains with deletions of both *myoB* and *myoE* result in hyperbranching and β-(1,3)-glucan patches throughout the hyphae. (C) MyoB is required for proper septum formation. Deletion of *myoB* resulted in malformed septa thicker than in the wild type. Septa were visualized using TEM. The arrowheads point to normal septa, and the dashed arrows indicate aberrant septa in the *myoB* deletion strain. (D) Strains harboring a deletion of *myoE* resulted in a significant radial-growth defect. Conidia (10^4) were spotted onto GMM agar and incubated for 5 days at 37°C. Radial growth was measured every 24 h. The error bars indicate standard errors of the means.

β-(1,3)-glucan (Fig. 1A). In contrast, the Δ*myoE* strain showed complete septa but small concentrated patches of chitin near some septal sites (Fig. 1A). Collectively, these data indicate that both *myoB* and *myoE* are important for proper assembly of cell wall components at the septum.

To better characterize the abnormal septa, TEM was performed on the wild-type and deletion strains (Fig. 1C). We visualized malformed septa in the Δ*myoB* strain and also noted that the Δ*myoB* septa were thicker than wild-type septa. Although the Δ*myoE* strain showed a severe radial-growth defect compared to the wild-type strain, its septa appeared normal. However, in the Δ*myoB* Δ*myoE* strain, no intact hyphae were present. It is possible that the sample preparation procedure for TEM may have caused hyphal lysis, but the mislocalization of β-(1,3)-glucan and lack of septation in the strain suggest cell wall defects. It remains unclear whether the β-(1,3)-glucan patches seen with aniline blue staining are improperly formed septa or mislocalized β-(1,3)-glucan.

Although TEM analysis did not show any defects in septal morphology in the Δ*myoE* strain, the deletion resulted in hyperseptation. To quantify this, we measured the apical and subapical hyphal compartments. Deletion of *myoE* resulted in a 2-fold decrease in apical-compartment size and in subapical-compartment size compared to the wild-type strain ($P < 0.001$), indicating that *myoE* is required for proper septal spacing (data not shown).

Deletion of *myoB* and double deletion of *myoB* and *myoE* results in increased sensitivity to cell wall stressors. To experimentally examine if the lack of septation and mislocalization of cell wall components in the mutant strains may be due to defective cell wall biosynthesis, we treated the myosin deletion strains with anti-cell wall agents. In comparison to the wild-type strain, the Δ*myoB* strain was more susceptible to the β-glucan synthase inhibitor caspofungin, but not to the chitin synthesis inhibitor nikkomycin Z (Fig. 2A). The Δ*myoB* Δ*myoE* strain failed to grow in the presence of caspofungin and was severely growth inhibited with nikkomycin Z (Fig. 2A). The Δ*myoE* strain showed equal growth in the presence or absence of anti-cell wall agents (Fig. 2A). However, when grown in liquid culture supplemented with caspofungin, these results slightly varied. The MEC was determined to be 0.125 μg/ml for the Δ*myoE* strain and 0.25 μg/ml for the Δ*myoB* strain, both slightly lower than that of the wild-type strain (0.5 μg/ml). *A. fumigatus* exhibits a phenomenon known as the paradoxical effect, in which a wild-type strain is growth inhibited at 0.5 to 2 μg/ml caspofungin but growth is remediated at 4 μg/ml caspofungin. While this paradoxical effect remained for the Δ*myoB* strain in solid medium (Fig. 2A), it was not recapitulated in liquid medium (Fig. 2B). The Δ*myoB* strain exhibited little growth from 0.5 μg/ml caspofungin up to 4 μg/ml caspofungin.

MyoB and MyoE localize to the septum, while only MyoE localizes to the hyphal tip. Because the morphological pheno-

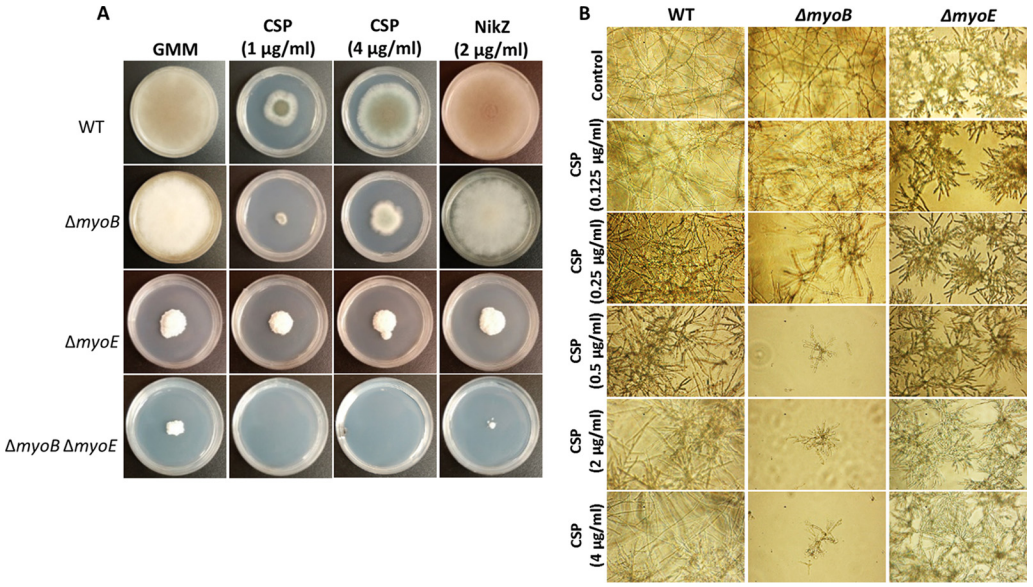

FIG 2 Myosin deletion strains are sensitive to anti-cell wall agents. (A) Deletion of *myoB* resulted in increased sensitivity to the β-(1,3)-glucan synthase inhibitor caspofungin (CSP) (1 μg/ml) but did not abolish paradoxical growth at 4 μg/ml CSP on plates. Deletion of both *myoB* and *myoE* resulted in increased sensitivity to both CSP and the chitin synthase inhibitor nikkomycin Z (NikZ). Conidia (10^4) were grown on GMM supplemented with the appropriate anti-cell wall drugs for 5 days at 37°C. (B) In liquid medium, deletion of *myoB* or *myoE* resulted in increased sensitivity to caspofungin, but only the Δ*myoB* strain exhibited loss of paradoxical growth. The MEC of caspofungin for the Δ*myoB* strain was 0.25 μg/ml and for the Δ*myoE* strain was 0.125 μg/ml. Conidia were grown in RPMI supplemented with the appropriate concentrations of caspofungin for 48 h at 37°C.

types of our *A. fumigatus* myosin deletion strains were different from those reported for *A. nidulans*, we speculated that there might be a variation in MyoB and MyoE localization. To examine this, we labeled MyoB and MyoE with GFP at their C termini and characterized their localization after 18 h of growth under standard conditions. The MyoB-enhanced green fluorescent protein (EGFP) fusion protein localized throughout the hyphae in ring-like structures, seemingly at future sites of septation, and in motile dot-like structures in the cytoplasm (Fig. 3A). MyoB was also observed in dot-like structures at some, but not all, mature septa; however, this localization pattern was rare and disappeared rapidly. MyoE, under the control of its native promoter, localized stably at the septa as two bars on either side of the septa, in nearly all hyphal tips, and in motile dot-like structures in the cytoplasm (Fig. 3B).

***myoE* is required for virulence in a *G. mellonella* and a murine model of invasive aspergillosis.** The pathogenesis of filamentous fungi is generally facilitated by penetration of host tissue through radial hyphal extension. Considering the lack of hyphal extension in the Δ*myoE* strain, we hypothesized that the strain might exhibit attenuated virulence. We first screened the myosin deletion strains in the heterologous invertebrate host *G. mellonella*. As expected, the Δ*myoE* strain was hypovirulent, with a nearly 50% higher survival rate 5 days after infection ($P < 0.0001$) than the wild-type strain (Fig. 4A). The Δ*myoB* strain showed decreased mortality, with a 40% higher survival rate ($P < 0.001$) despite radial hyphal extension similar to that of the wild-type strain (Fig. 4A).

Following screening in the *Galleria* model, we utilized a murine intranasal model of invasive aspergillosis and found that the Δ*myoB* and Δ*myoE* strains each showed decreased mortality compared to the wild-type strain in this second disease model ($P < 0.001$ and $P < 0.01$, respectively) (Fig. 4B).

Histopathological examination of murine lungs from mice at day +3 after infection demonstrated invasive hyphal growth in the wild-type and the Δ*myoE* strains yet little hyphal growth in the Δ*myoB* strain (Fig. 4C). Hematoxylin and eosin staining showed

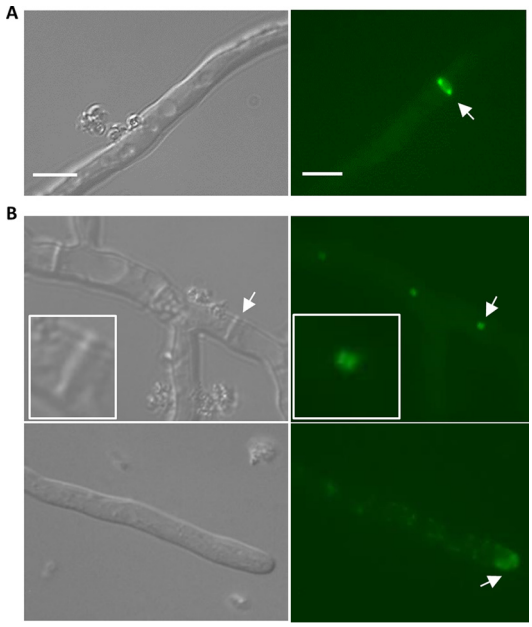

FIG 3 Localization of MyoB and MyoE. (A) MyoB localizes in rings in the hyphae. The arrow indicates the ring structure. (B) (Top) MyoE localizes to the fully formed septa as two discs on either side of it. (Bottom) MyoE localizes to the hyphal tip and in dot-like structures throughout the hyphae. (Insets) Enlargements of the arrow locations. The arrows indicate hyphal-tip and septum localization. Bar, 10 μm.

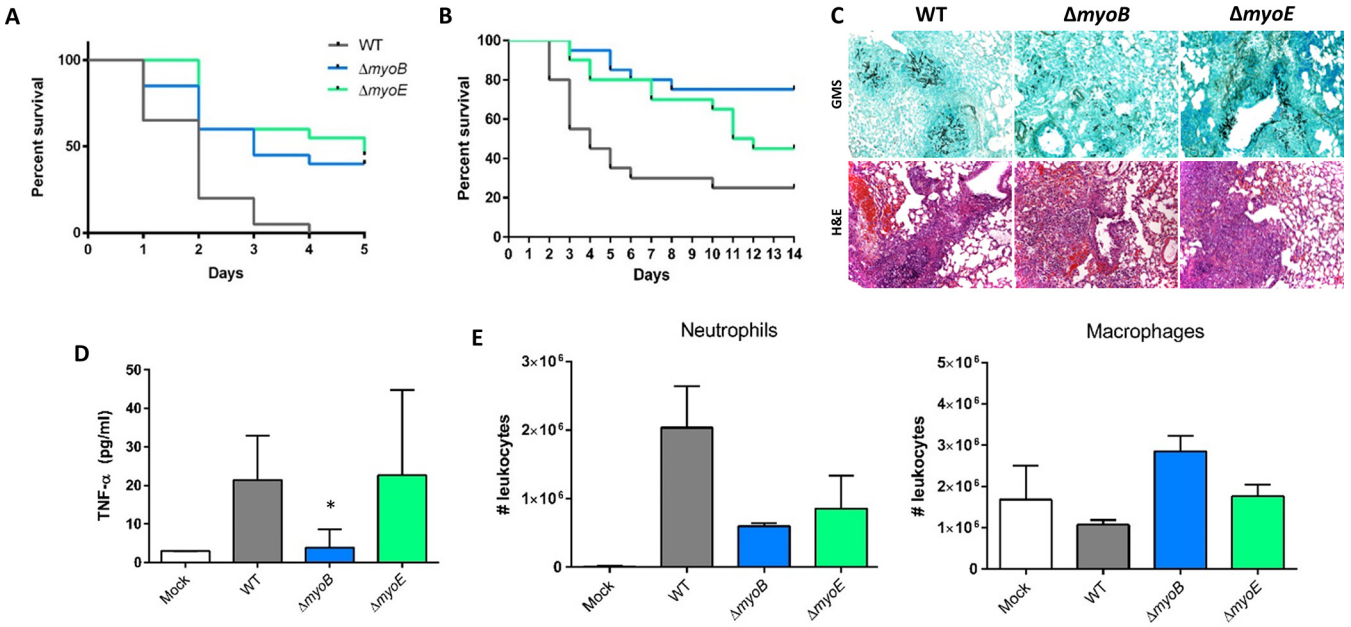

FIG 4 Effects of *myoB* and *myoE* deletion on virulence in the invertebrate host, *G. mellonella*, and in a murine model of invasive aspergillosis. (A) Conidia (5×10^6) were inoculated into an invertebrate host, *G. mellonella* larvae, and survival was scored every 24 h for 5 days. (B) Effect of *myoB* or *myoE* deletion on virulence in a persistently immunosuppressed murine model. Mice were immunosuppressed with cyclophosphamide and triamcinolone acetonide prior to infection. Conidia (4×10^6) were inoculated into the mice intranasally, and survival was scored every 24 h for 14 days. (C) Histopathological examination of the murine lungs 3 days after infection showed little fungal burden in the Δ*myoB* strain, while the wild-type and Δ*myoE* strains showed similar fungal burdens by Gomori methenamine silver stain (GMS). Inflammation was similar in the wild-type and single-deletion strains by hematoxylin and eosin (H&E). (D) BALF from infected mice was used to determine TNF-α release using ELISA. Mice infected with the Δ*myoB* strain released significantly less TNF-α than the wild-type or Δ*myoE* strain. (E) BALF from infected mice was used for leukocyte analysis by flow cytometry. *, $P < 0.05$ using an unpaired *t* test (compared to the WT). The error bars indicate standard errors of the means.

similar inflammation levels for both single-deletion strains compared to the wild-type strain (Fig. 4C).

The Δ*myoB* strain did not exhibit extensive fungal growth in the murine lung but did seem to elicit a pulmonary inflammatory response similar to that of the wild-type strain by H&E staining. Because H&E staining can be variable based on the different sections of the lung analyzed, we wanted to determine if the Δ*myoB* strain was immunoreactive using a more quantitative assay. To determine this, we collected bronchoalveolar lavage fluid from infected mice 3 days after infection. We measured the TNF-α released via ELISA and subjected the rest of the BALF to flow cytometry analysis. BALF collected from mice infected with the Δ*myoE* strain did not exhibit a significant difference in TNF-α release compared to the wild-type strain ($P > 0.9$); however, the mice infected with the Δ*myoB* strain showed a significant reduction in TNF-α release compared to those infected with the wild-type strain ($P < 0.05$) (Fig. 4D). Cellular analysis revealed that the percentages of leukocytes in the total cell population measured were similar for mock-infected mice and mice infected with all three strains. The vast majority of leukocytes were either neutrophils or macrophages, with macrophages being the primary leukocyte type in mock-infected mice (Fig. 4E). The total numbers of macrophages were similar for mice infected with the wild type, the Δ*myoE* strain, or the mock control; however, those infected with the Δ*myoB* strain showed statistically more macrophage infiltration than those infected with the wild-type strain ($P < 0.01$). Neutrophil infiltration was highest in mice infected with the wild-type strain, while those infected with either mutant strain showed decreased numbers of neutrophils.

Loss of myosins causes delayed germination, and loss of *myoB* results in decreased conidial viability. Due to the conidiation defect and lack of growth of the Δ*myoB* strain in the murine lung, we speculated that deletion of *myoB* might result in germination or conidial-viability deficiencies. As shown in Fig. 5A, all three myosin deletion strains showed significantly delayed germination compared to the wild-type strain, with the Δ*myoB* Δ*myoE* strain severely delayed. All three deletion strains failed to reach 100% germination.

To directly assess conidial viability, conidia from the wild-type strain and all three myosin deletion strains were stained with DiBAC and CFDA, which stain dead and live cells, respectively (34, 35). While the Δ*myoE* strain showed no conidial-viability defects, the Δ*myoB* strain exhibited a greater-than-2-fold increase in nonviable conidia compared to the wild-type strain ($P < 0.05$), shown using complementary stains, suggesting that *myoB* is important for preserving conidial viability (Fig. 5B and C). Based on this result, we consider that the decreased mortality and fungal burden observed with infection with the Δ*myoB* strain are likely due to reduced conidial viability. Unfortunately, attempts to reevaluate virulence with equivalent numbers of viable Δ*myoB* conidia, normalized to the number of conidia used for infections with the Δ*myoE* and wild-type strains, was not technically possible due to a higher conidial concentration interfering with safe murine intranasal inoculation. The Δ*myoB* Δ*myoE* double-deletion strain could not be quantified for conidial viability because the conidia could not be pelleted upon centrifugation. Because conidia were produced in the mutant strains only in the presence of sorbitol, an osmotic stabilizer, we also wanted to determine if

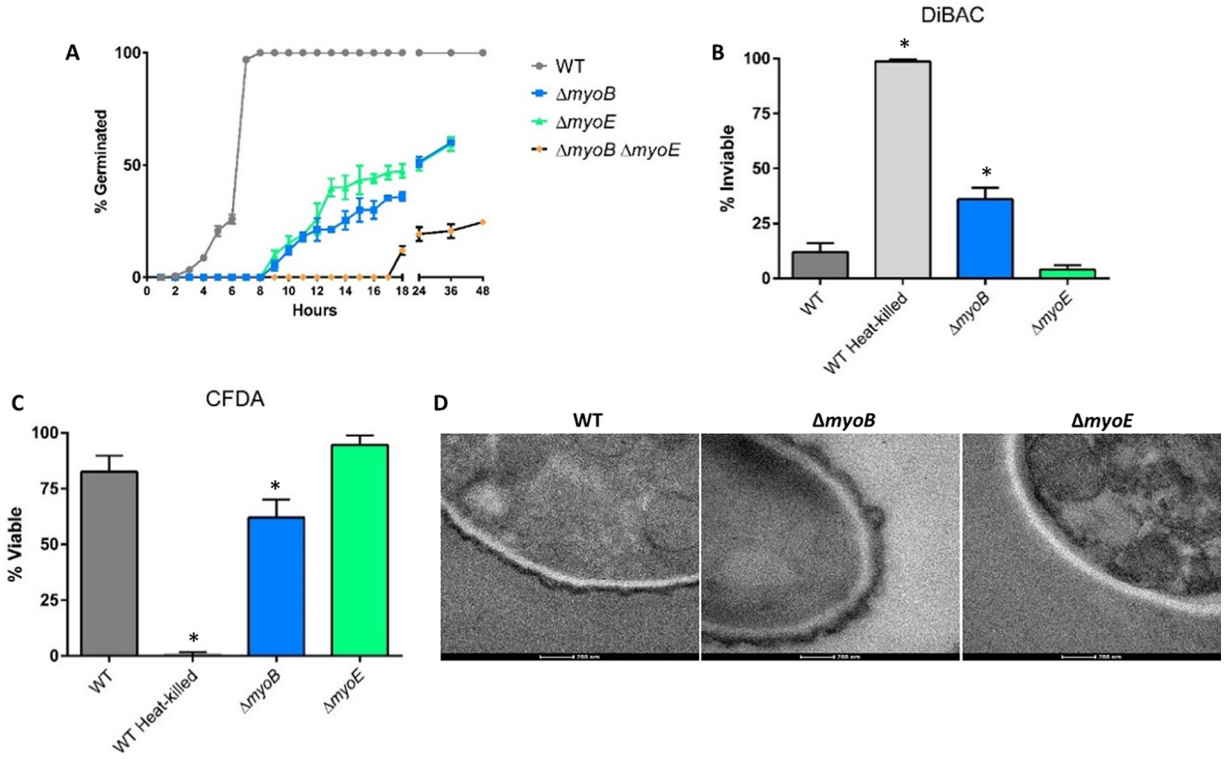

FIG 5 Myosins are required for conidial germination. (A) Conidia (~100) were inoculated into GMM, grown at 37°C, and quantified as germinated or not using a Nikon Diaphot phase-contrast microscope at the indicated time points. (B and C) Conidia were stained with DiBAC (B) or CFDA (C) and quantified by fluorescence microscopy. (D) Deletion of *myoB* results in conidia with a thicker electron-dense outer layer, while deletion of *myoE* results in conidia lacking this layer. The conidia were visualized by TEM. *, $P < 0.05$ using an unpaired *t* test (compared to the WT). The error bars indicate standard errors of the means.

harvesting and storing conidia in water had an effect on viability. We harvested and diluted conidia in water or PBS and then performed the viability staining with DiBAC and CFDA as previously described. The staining revealed that conidia harvested in either water or PBS resulted in no statistically different viability for any strains (see Fig. S2 in the supplemental material).

In order to determine if the myosin deletion strains might have defects in the conidial-wall surface which could trigger greater immune response or nonviability, we performed TEM on the Δ*myoB* and Δ*myoE* conidia (Fig. 5D). The Δ*myoB* conidia showed an electron-dense outer layer that in some instances looked thicker than that of the wild-type strain. This heterogeneity in phenotype was not seen in the wild-type strain. In contrast, the Δ*myoE* conidia generally showed no electron-dense outer layer.

DISCUSSION

Myosins are involved in diverse and critical cellular processes and thus are paramount for understanding fungal growth, septation, and virulence, which may lead to future antifungal targeting. We conducted the first genetic characterization of the class II and class V myosin genes in *A. fumigatus* (*myoB* and *myoE*, respectively). *myoB* is required for normal septation, as deletion of *myoB* resulted in significant lateral or central joining defects. MyoB also localized transiently to the septa and in rings in the hyphae at presumed sites of septation, consistent with MyoB's known role as part of the actin-myosin ring to form septa (5, 21, 36–38). In contrast to the Δ*myoB* strain in *A. nidulans*, *A. fumigatus myoB* is dispensable for radial growth, thus displaying diverse functional contributions within the same genus (5).

Deletion of *myoE* resulted in significant loss of radial growth, hyperbranching, and loss of hyphal polarity, demonstrating the role of *myoE* in maintaining apical dominance. Class V myosins are known to be vesicle traffickers to the hyphal tip (5, 19, 23, 24); thus, the loss of *myoE* likely results in improper trafficking, and components necessary for hyphal extension may diffuse to nonspecific areas, causing hyperbranching and loss of polarity. The class V myosin's role in septation is unknown, but our data imply a role for *myoE* in maintaining the regular frequency of septation. MyoE under its native promoter localizes stably to every septum, so it is possible that MyoE serves as a marker for fully formed septa to modulate the frequency of septation.

A. fumigatus MyoB and MyoE have important roles in conidial production, germination, and conidial viability. Loss of *myoB* resulted in reduced conidial viability and delayed germination. Although most conidia remained viable in the Δ*myoE* strain, conidial germination reached only approximately 50% by 36 h. The emergence of a germ tube during conidial germination is known to involve polarization proteins, as well as the vesicle-trafficking system (39–42). Thus, deletion of *myoE* may result in live conidia but also the inability of the conidia to properly establish polarity to initiate germination.

Myosins are also needed for proper cell wall component distribution. The Δ*myoB* Δ*myoE* strain exhibited β-(1,3)-glucan mislocalization throughout the cytoplasm; in contrast, the Δ*myoB* strain exhibited aberrant accumulation of β-(1,3)-glucan only at septal sites, while the Δ*myoE* strain showed normal β-(1,3)-glucan localization. In contrast to β-(1,3)-glucan localization, the

Δ*myoE* strain exhibited slight accumulation of chitin as small patches that were usually near septa. In *S. cerevisiae*, loss of *myo2* resulted in chitin mislocalization, and Myo2p is required to traffic Chs3p, a chitin synthase enzyme, to the proper locations (43). Our data indicate that a similar system may exist in *A. fumigatus*.

The Δ*myoB* and Δ*myoE* strains resulted in reduced mortality in both *Galleria* and murine models of invasive aspergillosis compared to the wild-type strain. The attenuated virulence of the Δ*myoE* strain is likely due to impaired radial growth, but the Δ*myoB* strain has growth similar to that of the wild-type strain *in vitro*. Histopathological analyses showed that the Δ*myoB* strain grows less than the Δ*myoE* strain and the wild-type strain in the murine lung. Significantly lower conidial germination and viability of the Δ*myoB* strain are most likely the cause of the reduced mortality and fungal burden. While the Δ*myoB* strain exhibits less fungal burden in the murine lung, the strain still elicits a pulmonary inflammatory response similar to that of the wild-type strain, as seen by H&E staining. We measured TNF-α release of BALF from infected mice 3 days after infection to determine if an *in vivo* analysis could recapitulate our histopathology results. Mice infected with the Δ*myoB* strain elicited reduced TNF-α release compared to the wild type, most likely due to the decreased fungal burden at day 3, and to Δ*myoE* strains, indicating that the Δ*myoB* strain is not more immunoreactive or the increase in the signal for inflammation precedes day 3 after infection, such as when spores are in contact with the lung epithelium, and thus, we were not able capture this due to the time course. Cellular analysis of the lung showed that more macrophages were present in mice infected with the Δ*myoB* strain while fewer neutrophils were present in mice infected with either mutant strain compared to the wild-type strain. Neutrophils are primarily responsible for hyphal killing (44), and therefore, one would expect to see fewer neutrophils present in those strains that have hyphal defects or grow less in murine lungs, such as both mutant strains. On the other hand, macrophages are a primary defense against invading conidia (45); therefore, deletion of *myoB* could result in disorganization of the conidial cell wall that leads to an increase in macrophage infiltration. This is in agreement with the inflammation seen in the H&E staining and the cellular infiltration analysis. TEM analysis revealed that the electron-dense outer layer of Δ*myoB* conidia was intact, albeit thicker, and might have disproportionate cell wall material, aiding an increase in immune response. On the other hand, TEM of Δ*myoE* conidia revealed the absence of an electron-dense outer layer, suggesting that (i) MyoE is required for its production or (ii) deletion of *myoE* reduces the structural rigidity/attachment of the layer, which is detached through vigorous washing and staining.

In conclusion, we have shown the important but distinct roles that class II and class V myosins have in maintaining proper hyphal morphology and disease pathogenesis in *A. fumigatus*. Both the class II myosin (MyoB) and the class V myosin (MyoE) are required for septation, conidiation, and conidial germination. MyoB is necessary for proper conidial viability, while MyoE is required for radial growth, hyphal polarity, chitin distribution, and virulence. Furthermore, we have demonstrated that class V myosins have a role in septation, as has been found in other fungi. Based on these findings, determining the cell wall composition of the conidia of the myosin deletion strains may provide clues leading to the varied immune reactions, and the identification of class V myosin interactants may help reveal its specific role in septation in filamentous fungi.

ACKNOWLEDGMENTS

We acknowledge Andrew Alspaugh's laboratory (Duke University) for helpful technical support and discussion of experimental design, Michelle Gignac Plue (Duke University) for assistance in performing transmission electron microscopy, and Dee Gunn's laboratory (Duke University) for assistance in performing flow cytometry.

Any opinions, findings, and conclusions expressed in this publication are ours and do not necessarily reflect the views of the National Science Foundation or NIH.

FUNDING INFORMATION

This work, including the efforts of William J. Steinbach, was funded by NIH (1 R01 AI112595-01). This work, including the efforts of José M. Vargas-Muñiz, was funded by National Science Foundation (NSF) (DGF 1106401).

REFERENCES

1. **McGoldrick CA, Gruver C, May GS.** 1995. *myoA* of *Aspergillus nidulans* encodes an essential myosin I required for secretion and polarized growth. J Cell Biol **128:**577–587. http://dx.doi.org/10.1083/jcb.128.4.577.
2. **Ali MY, Krementsova EB, Kennedy GG, Mahaffy R, Pollard TD, Trybus KM, Warshaw DM.** 2007. Myosin Va maneuvers through actin intersections and diffuses along microtubules. Proc Natl Acad Sci U S A **104:**4332–4336. http://dx.doi.org/10.1073/pnas.0611471104.
3. **Osherov N, Yamashita RA, Chung YS, May GS.** 1998. Structural requirements for in vivo myosin I function in *Aspergillus nidulans*. J Biol Chem **273:**27017–27025. http://dx.doi.org/10.1074/jbc.273.41.27017.
4. **Steinberg G.** 2007. Hyphal growth: a tale of motors, lipids, and the Spitzenkörper. Eukaryot Cell **6:**351–360. http://dx.doi.org/10.1128/EC.00381-06.
5. **Taheri-Talesh N, Xiong Y, Oakley BR.** 2012. The functions of myosin II and myosin V homologs in tip growth and septation in *Aspergillus nidulans*. PLoS One **7:**e31218. http://dx.doi.org/10.1371/journal.pone.0031218.
6. **Xiang X, Plamann M.** 2003. Cytoskeleton and motor proteins in filamentous fungi. Curr Opin Microbiol **6:**628–633. http://dx.doi.org/10.1016/j.mib.2003.10.009.
7. **Zhang J, Tan K, Wu X, Chen G, Sun J, Reck-Peterson SL, Hammer JA, III, Xiang X.** 2011. *Aspergillus* myosin-V supports polarized growth in the absence of microtubule-based transport. PLoS One **6:**e28575. http://dx.doi.org/10.1371/journal.pone.0028575.
8. **Berg JS, Powell BC, Cheney RE.** 2001. A millennial myosin census. Mol Biol Cell **12:**780–794. http://dx.doi.org/10.1091/mbc.12.4.780.
9. **Geli MI, Riezman H.** 1996. Role of type I myosins in receptor-mediated endocytosis in yeast. Science **272:**533–535. http://dx.doi.org/10.1126/science.272.5261.533.
10. **Giblin J, Fernandez-Golbano IM, Idrissi FZ, Geli MI.** 2011. Function and regulation of *Saccharomyces cerevisiae* myosins-I in endocytic budding. Biochem Soc Trans **39:**1185–1190. http://dx.doi.org/10.1042/BST0391185.
11. **Lister IM, Tolliday NJ, Li R.** 2006. Characterization of the minimum domain required for targeting budding yeast myosin II to the site of cell division. BMC Biol **4:**19. http://dx.doi.org/10.1186/1741-7007-4-19.
12. **Liu X, Osherov N, Yamashita R, Brzeska H, Korn ED, May GS.** 2001. Myosin I mutants with only 1% of wild-type actin-activated MgATPase activity retain essential in vivo function(s). Proc Natl Acad Sci U S A **98:**9122–9127. http://dx.doi.org/10.1073/pnas.161285698.
13. **Reck-Peterson SL, Tyska MJ, Novick PJ, Mooseker MS.** 2001. The yeast class V myosins, Myo2p and Myo4p, are nonprocessive actin-based motors. J Cell Biol **153:**1121–1126. http://dx.doi.org/10.1083/jcb.153.5.1121.
14. **Takeshita N, Yamashita S, Ohta A, Horiuchi H.** 2006. *Aspergillus nidulans* class V and VI chitin synthases CsmA and CsmB, each with a myosin motor-like domain, perform compensatory functions that are essential for hyphal tip growth. Mol Microbiol **59:**1380–1394. http://dx.doi.org/10.1111/j.1365-2958.2006.05030.x.
15. **Yamashita RA, May GS.** 1998. Constitutive activation of endocytosis by mutation of *myoA*, the myosin I gene of *Aspergillus nidulans*. J Biol Chem **273:**14644–14648. http://dx.doi.org/10.1074/jbc.273.23.14644.

16. **Goodson HV, Anderson BL, Warrick HM, Pon LA, Spudich JA.** 1996. Synthetic lethality screen identifies a novel yeast myosin I gene (MYO5): myosin I proteins are required for polarization of the actin cytoskeleton. J Cell Biol **133:**1277–1291. http://dx.doi.org/10.1083/jcb.133.6.1277.
17. **Goodson HV, Spudich JA.** 1995. Identification and molecular characterization of a yeast myosin I. Cell Motil Cytoskeleton **30:**73–84. http://dx.doi.org/10.1002/cm.970300109.
18. **Haarer BK, Petzold A, Lillie SH, Brown SS.** 1994. Identification of MYO4, a second class V myosin gene in yeast. J Cell Sci **107:**1055–1064.
19. **Johnston GC, Prendergast JA, Singer RA.** 1991. The *Saccharomyces cerevisiae* MYO2 gene encodes an essential myosin for vectorial transport of vesicles. J Cell Biol **113:**539–551. http://dx.doi.org/10.1083/jcb.113.3.539.
20. **Watts FZ, Shiels G, Orr E.** 1987. The yeast MYO1 gene encoding a myosin-like protein required for cell division. EMBO J **6:**3499–3505.
21. **Bi E, Maddox P, Lew DJ, Salmon ED, McMillan JN, Yeh E, Pringle JR.** 1998. Involvement of an actomyosin contractile ring in *Saccharomyces cerevisiae* cytokinesis. J Cell Biol **142:**1301–1312. http://dx.doi.org/10.1083/jcb.142.5.1301.
22. **Canovas D, Boyce KJ, Andrianopoulos A.** 2011. The fungal type II myosin in *Penicillium marneffei*, MyoB, is essential for chitin deposition at nascent septation sites but not actin localization. Eukaryot Cell **10:**302–312. http://dx.doi.org/10.1128/EC.00201-10.
23. **Govindan B, Bowser R, Novick P.** 1995. The role of Myo2, a yeast class V myosin, in vesicular transport. J Cell Biol **128:**1055–1068. http://dx.doi.org/10.1083/jcb.128.6.1055.
24. **Hammer JA, III, Sellers JR.** 2012. Walking to work: roles for class V myosins as cargo transporters. Nat Rev Mol Cell Biol **13:**13–26. http://dx.doi.org/10.1038/nrm3248.
25. **Woo M, Lee K, Song K.** 2003. MYO2 is not essential for viability, but is required for polarized growth and dimorphic switches in *Candida albicans*. FEMS Microbiol Lett **218:**195–202. http://dx.doi.org/10.1111/j.1574-6968.2003.tb11518.x.
26. **Weber I, Gruber C, Steinberg G.** 2003. A class-V myosin required for mating, hyphal growth, and pathogenicity in the dimorphic plant pathogen *Ustilago maydis*. Plant Cell **15:**2826–2842. http://dx.doi.org/10.1105/tpc.016246.
27. **Steinbach WJ, Cramer RA, Jr, Perfect BZ, Asfaw YG, Sauer TC, Najvar LK, Kirkpatrick WR, Patterson TF, Benjamin DK, Jr, Heitman J, Perfect JR.** 2006. Calcineurin controls growth, morphology, and pathogenicity in *Aspergillus fumigatus*. Eukaryot Cell **5:**1091–1103. http://dx.doi.org/10.1128/EC.00139-06.
28. **Juvvadi PR, Fortwendel JR, Rogg LE, Burns KA, Randell SH, Steinbach WJ.** 2011. Localization and activity of the calcineurin catalytic and regulatory subunit complex at the septum is essential for hyphal elongation and proper septation in *Aspergillus fumigatus*. Mol Microbiol **82:**1235–1259. http://dx.doi.org/10.1111/j.1365-2958.2011.07886.x.
29. **Langfelder K, Philippe B, Jahn B, Latge JP, Brakhage AA.** 2001. Differential expression of the *Aspergillus fumigatus pksP* gene detected in vitro and in vivo with green fluorescent protein. Infect Immun **69:**6411–6418. http://dx.doi.org/10.1128/IAI.69.10.6411-6418.2001.
30. **Lamoth F, Juvvadi PR, Fortwendel JR, Steinbach WJ.** 2012. Heat shock protein 90 is required for conidiation and cell wall integrity in Aspergillus fumigatus. Eukaryot Cell **11:**1324–1332. http://dx.doi.org/10.1128/EC.00032-12.
31. **Fortwendel JR, Juvvadi PR, Pinchai N, Perfect BZ, Alspaugh JA, Perfect JR, Steinbach WJ.** 2009. Differential effects of inhibiting chitin and 1,3-{beta}-D-glucan synthesis in ras and calcineurin mutants of Aspergillus fumigatus. Antimicrob Agents Chemother **53:**476–482. http://dx.doi.org/10.1128/AAC.01154-08.
32. **CLSI.** 2008. Reference method for broth dilution antifungal susceptibility testing of filamentous fungi; approved standard, 2nd ed. CLSI, Wayne, PA.
33. **Steinbach WJ, Benjamin DK, Jr, Trasi SA, Miller JL, Schell WA, Zaas AK, Foster WM, Perfect JR.** 2004. Value of an inhalational model of invasive aspergillosis. Med Mycol **42:**417–425. http://dx.doi.org/10.1080/13693780410001712034.
34. **Belaish R, Sharon H, Levdansky E, Greenstein S, Shadkchan Y, Osherov N.** 2008. The Aspergillus nidulans cetA and calA genes are involved in conidial germination and cell wall morphogenesis. Fungal Genet Biol **45:**232–242. http://dx.doi.org/10.1016/j.fgb.2007.07.005.
35. **Bowman JC, Hicks PS, Kurtz MB, Rosen H, Schmatz DM, Liberator PA, Douglas CM.** 2002. The antifungal echinocandin caspofungin acetate kills growing cells of Aspergillus fumigatus in vitro. Antimicrob Agents Chemother **46:**3001–3012. http://dx.doi.org/10.1128/AAC.46.9.3001-3012.2002.
36. **Hill TW, Jackson-Hayes L, Wang X, Hoge BL.** 2015. A mutation in the converter subdomain of *Aspergillus nidulans* MyoB blocks constriction of the actomyosin ring in cytokinesis. Fungal Genet Biol **75:**72–83. http://dx.doi.org/10.1016/j.fgb.2015.01.010.
37. **Mulvihill DP, Hyams JS.** 2003. Role of the two type II myosins, Myo2 and Myp2, in cytokinetic actomyosin ring formation and function in fission yeast. Cell Motil Cytoskeleton **54:**208–216. http://dx.doi.org/10.1002/cm.10093.
38. **Song B, Li HP, Zhang JB, Wang JH, Gong AD, Song XS, Chen T, Liao YC.** 2013. Type II myosin gene in *Fusarium graminearum* is required for septation, development, mycotoxin biosynthesis and pathogenicity. Fungal Genet Biol **54:**60–70. http://dx.doi.org/10.1016/j.fgb.2013.02.010.
39. **d'Enfert C.** 1997. Fungal spore germination: insights from the molecular genetics of *Aspergillus nidulans* and *Neurospora crassa*. Fungal Genet Biol **21:**163–172. http://dx.doi.org/10.1006/fgbi.1997.0975.
40. **Harris SD.** 2006. Cell polarity in filamentous fungi: shaping the mold. Int Rev Cytol **251:**41–77. http://dx.doi.org/10.1016/S0074-7696(06)51002-2.
41. **Harris SD, Momany M.** 2004. Polarity in filamentous fungi: moving beyond the yeast paradigm. Fungal Genet Biol **41:**391–400. http://dx.doi.org/10.1016/j.fgb.2003.11.007.
42. **Momany M.** 2002. Polarity in filamentous fungi: establishment, maintenance and new axes. Curr Opin Microbiol **5:**580–585. http://dx.doi.org/10.1016/S1369-5274(02)00368-5.
43. **Santos B, Snyder M.** 1997. Targeting of chitin synthase 3 to polarized growth sites in yeast requires Chs5p and Myo2p. J Cell Biol **136:**95–110. http://dx.doi.org/10.1083/jcb.136.1.95.
44. **Park SJ, Mehrad B.** 2009. Innate immunity to Aspergillus species. Clin Microbiol Rev **22:**535–551. http://dx.doi.org/10.1128/CMR.00014-09.
45. **Philippe B, Ibrahim-Granet O, Prevost MC, Gougerot-Pocidalo MA, Sanchez Perez M, Van der Meeren A, Latge JP.** 2003. Killing of Aspergillus fumigatus by alveolar macrophages is mediated by reactive oxidant intermediates. Infect Immun **71:**3034–3042. http://dx.doi.org/10.1128/IAI.71.6.3034-3042.2003.
46. **da Silva Ferreira ME, Kress MRVZ, Savoldi M, Goldman MHS, Härtl A, Heinekamp T, Brakhage AA, Goldman GH.** 2006. The *akuB*^{KU80} mutant deficient for nonhomologous end joining is a powerful tool for analyzing pathogenicity in *Aspergillus fumigatus*. Eukaryot Cell **5:**207–211. http://dx.doi.org/10.1128/EC.5.1.207-211.2006.